Multi-scale laminar flows with turbulent-like properties

Lionel Rossi, J.C. Vassilicos* and Yannis Hardalupas†
Imperial College London, London SW7 2AZ, United Kingdom
(Dated: June 29, 2006)

By applying fractal electromagnetic force fields on a thin layer of brine, we generate steady quasi-two-dimensional laminar flows with multi-scale stagnation point topology. This topology is shown to control the evolution of pair separation (Δ) statistics by imposing a turbulent-like locality based on the sizes and strain rates of hyperbolic stagnation points when the flows are fast enough, in which case $\overline{\Delta^2} \sim t^\gamma$ is a good approximation with γ close to 3. Spatially multi-scale laminar flows with turbulent-like spectral and stirring properties are a new concept with potential applications in efficient and micro-fluidic mixing.

PACS numbers: 47.27 -i and 47.62 +q

I. INTRODUCTION

The rate with which pairs of points separate in phase or physical space is of central importance to dynamical systems. In turbulent flows, pairs of fluid elements (also refered to as particles here) separate algebraically [1–10]. As originally pointed out in [1], their statistics bare the imprint of the entire range of turbulent eddy scales. A theory has been developed recently which relates turbulent pair diffusion statistics to the multi-scale streamline topology of the turbulence, specifically to its multi-scale stagnation point structure [4–6, 11, 12]. This theory is based on the picture, originally conjectured by [2], that in turbulent flows, fluid element pairs travel together for long times and separate suddenly when they encounter a straining stagnation point. Recent laboratory experiments have confirmed that pairs travel together for long and separate in sudden bursts [3].

This new theory has been formulated for isotropic homogeneous turbulence and its central tenet is that stagnation points in the frame where the mean flow is zero are persistent enough on average to dominate the average separation rate of fluid element pairs. The rational for this tenet is that pairs are subjected to a sustained exponential separation rate at persistent straining stagnation points as can occur nowhere else in the flow. The statistical persistence of these points has been established by Direct Numerical Simulations and by theoretical argumentation [11, 12]. The second important tenet of the theory is that straining stagnation points have a length-scale associated with them. Hence, the Richardson locality hypothesis that the pair separation rate is dominated by eddies of length-scale comparable to the pair's separation can be rephrased by replacing "eddies" with "straining stagnation points". This Richardson-type locality is a very broad concept because a wide range of power law energy spectra can lead to power law pair separation [4].

Due to the impossibility (at least by current means), to monitor and measure in the laboratory the multi-scale topology of the turbulence on the fly and its instantaneous links to pair diffusion (i.e. identify most stagnation points and follow their paths whilst measuring their length-scales and following fluid element pairs at the same time), we propose to test this new theory in bespoke multi-scale flows with electromagnetically imposed turbulent-like multi-scale stagnation point topology following the recent work of [13]. An important first case of such bespoke multi-scale flow design is the case of the steady quasi-two-dimensional (Q2D) laminar flow. If non-trivial statistics of pair diffusion exist in such a flow they must necessarily result from the flow's multi-scale stagnation point topology. Furthermore, multi-scale laminar flows with turbulent-like properties are a new concept with potential applications in micro-fluidic and efficient mixers. Unlike chaotic advection [14], these flows are spatially multi-scale. It is our purpose here to study pair diffusion statistics in such flows and investigate the relations of these statistics to the flow's multi-scale stagnation point topology. It is therefore also our purpose to measure and characterise this multi-scale stagnation point structure, in part by introducing a measurable definition of stagnation point length-scale.

II. MULTI-SCALE FLOW AND ITS STAGNATION POINT STRUCTURE

[4] and [5] showed that, in 2D turbulent flows with an energy spectrum $E(k) \sim k^{-p}$ where $p < 3$, the multi-scale streamline topology consists of cat's eyes within cat's eyes (see figure 1b) which implies a fractal-like distribution of stagnation points. [6] showed that the number density n_s of stagnation points is a power-law function of the outer to inner length-scale ratio L/η, $n_s = C_s L^{-d}(L/\eta)^{Ds}$ where the fractal dimension D_s is such that $p + 2D_s/d = 3$ and d=2, 3 for 2D, 3D turbulence. [13] generated a Q2D multi-scale laminar flow with an imposed multi-scale spatial distribution of stagnation points and corroborated that such a flow has a power-law energy spectrum in agreement with $p + D_s = 3$. The same rig and family of flows ($p \approx 2.5$) are used here.

*Department of Aeronautics; Electronic address: rossi_lionel@yahoo.fr;j.c.vassilicos@imperial.ac.uk
†Department of Mechanical Engineering; Electronic address: y.hardalupas@imperial.ac.uk

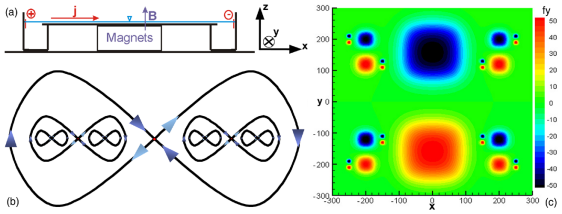

FIG. 1: (a) Schematic of rig; (b) Schematic of multi-scale flow based on a 8 in 8 topology, (c) Electromagnetic forcing distribution computed for our spatial distribution of multi-sized magnets (I=1A, B=1T; f_y in N/m^3; x and y in mm).

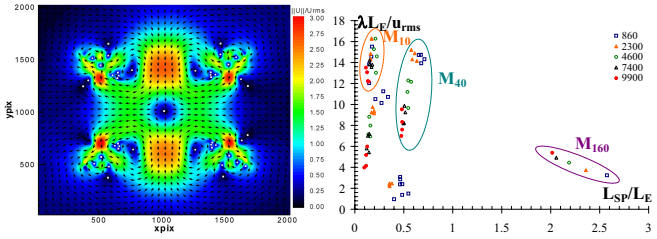

FIG. 2: (a) PIV velocity field ($\mathbf{u}/\mathbf{u_{rms}}$, 1/64 arrows), Re_{2D} = 600, squares refer to hyperbolic stagnation points, disks to elliptic stagnation points; (b) scatter plot of hyperbolic stagnation point strain rates, $\lambda L_E/u_{rms}$, and sizes, L_S/L_E.

A. Experimental set-up and flow

Figure 1a is a schematic of the rig. An horizontal shallow layer of brine (NaCl,158g/l, thickness H=5mm) is forced by a fractal distribution of opposite pairs of Lorentz forces as shown in figure 1c. These electromagnetic (EM) forces are generated by an electric current through the brine and permanent magnets of various horizontal sizes (10mm, 40mm, 160mm) placed under the bottom wall which supports the brine.

The two-component velocity field $\mathbf{u}(\mathbf{x},t)$ at the free surface of the brine layer generated by these fractal EM forces has been measured by Particle Image Velocimetry (PIV), using a 14Hz, 14bit, 2048x2048 $pixel^2$ camera. The flow is measured in a large square frame (which cover all magnets) of size $L_{PIV} = 813.4mm$ which is small compared to the size of the tank ($1700 \times 1700mm^2$). The physical length of one pixel is about 0.3972mm. The correlation windows have 16×16 pixels (search window 42×42 pixels), and the overlap in each direction is of 9 pixels. This leads to a measurement grid containing 287x287 velocity vectors. For full details on the rig and experiments, see [13] who also show that the flow at the free surface of the brine is Q2D.

With steady EM forces the flows are stationary after an initial transient following the sudden switch-on of the forces. A Reynolds number $Re_{2D} = u_{rms}L_{PIV}/\nu$ is defined based on L_{PIV}, the root mean square of the PIV velocity field, u_{rms}, (which is controlled by varying the intensity of the electric current), and the kinematic viscosity of the brine, ν. In this letter we present results obtained for eleven different values of Re_{2D} from 600 to 9900. Even though the values of Re_{2D} are large, all these flows are Q2D as shown in [13] and laminar as they present no instabilities and the fluid velocity values are never larger than a few cm/s.

The velocity fields are very similar over the entire range of Reynolds numbers. Indeed, the spatial correlation between two velocity fields $\mathbf{u_1}$ and $\mathbf{u_2}$ obtained at two different Reynolds numbers is always larger than 0.84 with an average of 0.947 and a standard deviation of 4.5%. Integral length scales, L_E, are obtained from the spatial auto-correlation of the velocity fields and their values slowly increase from about $16cm$ to about $20cm$ as Re_{2D} increases from 600 to 9900. This increase of L_E reflects the slight increase of the largest eddy size.

B. Multi-scale stagnation point structure

The stagnation point positions, $\mathbf{x}_s$, are obtained with a Newton-Raphson algorithm applied to the PIV velocity field, see figure 2a. The flow being incompressible, stagnation points are characterised by a single positive strain or rotation rate, λ (in 1/s), which is an eigenvalue of $J_{ij} = \partial u_i/\partial x_j$ at the stagnation point: the eigenvalues and eigenvectors $\mathbf{X}$ are given by $\mathbf{JX} = \pm\lambda\mathbf{X}$ for hyperbolic stagnation points or $\mathbf{JX} = \pm\mathbf{i}\lambda\mathbf{X}$ for elliptic ones.

Hyperbolic stagnation points also have an associated length-scale L_s which, in 2D incompressible flow, scales with the size of the streamlines emanating from or passing very close to them. To define and calculate L_s we integrate the velocity $\mathbf{u}$ (obtained from our PIV and Lagrange interpolation within the PIV grid) along a streamline starting from a point $\mathbf{x}_s + \epsilon\mathbf{e}_\theta$ very close to a hyperbolic stagnation point $\mathbf{x}_s$ (ϵ is very small, within the size of the PIV grid) and $\mathbf{e}_\theta$ is a unit vector of angle θ. We track the value of $\mathbf{u}\cdot\mathbf{e}_\theta$ while integrating along the streamline and record the point $\mathbf{x_l}(\theta)$ where this quantity changes sign. We then define $L_s \equiv \langle|\mathbf{x_l}(\theta) - \mathbf{x}_s|\rangle_\theta$, where the averaging operation $\langle ...\rangle_\theta$ is over θ. L_s is a measure of the characteristic distance from $\mathbf{x}_s$ where streamlines passing very close to $\mathbf{x}_s$ take a turn.

We calculated L_s for all the hyperbolic stagnation points at various values of Re_{2D}. Figure 2b is a scatter plot of the strain rates λ and the stagnation point sizes L_s for all hyperbolic points and five different values of Re_{2D}. The hyperbolic stagnation points directly imposed by the EM forcing between the magnets (which correspond with stagnation points of the forcing, see figures 1b and 2a) are circled and marked with the corresponding scale of forcing: M_{10}, M_{40}, M_{160}. It is found that the length-scales L_s cluster around three values L_{s3}, L_{s2} and L_{s1} separated by an approximate factor 4 from each other. This factor corresponds to the ratio 4 between the different magnet sizes.

In figure 3 we plot the three mean values of λ averaged over the hyperbolic points directly imposed by the EM forcing. These mean values are respectively denoted

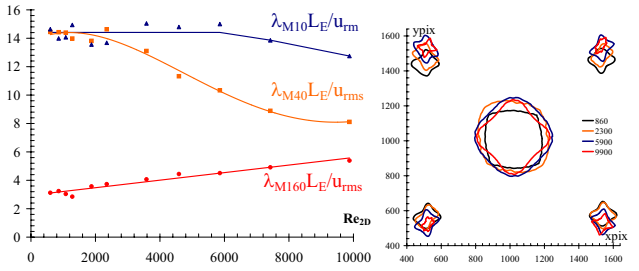

FIG. 3: Left: Dimensionless mean stagnation point strain rates versus Re_{2D}. Right: Areas of direct influence of stagnation points related to M_{160} and M_{40} for various Re_{2D}.

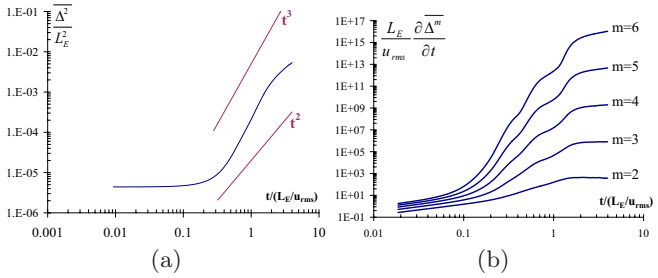

FIG. 4: Two-particle dispersion, $Re_{2D} = 7400$, (a) $\overline{\Delta^2}/L_E^2$ (b), $\frac{L_E}{u_{rms}}\frac{\partial\overline{\Delta^m}}{\partial t}$.

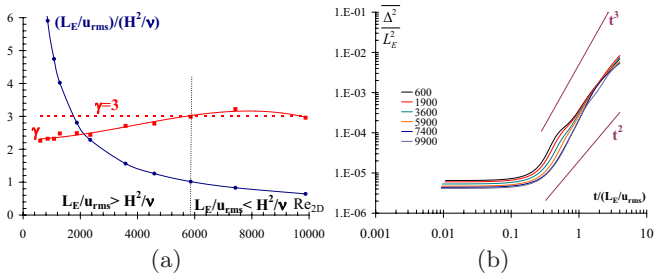

FIG. 5: (a) Ridchardson-like exponent, γ, ($\overline{\Delta^2} \sim t^\gamma$) and ratio L_E/u_{rms} to H^2/ν as function of Re_{2D} ; (b) two-particle dispersion, $\overline{\Delta^2}/L_E^2$, various Re_{2D}.

$\lambda_3 = \lambda_{M10}$, $\lambda_2 = \lambda_{M40}$ and $\lambda_1 = \lambda_{M160}$, and correspond to length-scales M_{10}, M_{40} and M_{160} which themselves correspond to the characteristic stagnation point scales L_s denoted L_{s_3}, L_{s_2}, L_{s_1} respectively. In figure 3, λ_3, λ_2 and λ_1 are normalised by u_{rms}/L_E and are plotted against Re_{2D}. We observe that a clear multi-scale structure appears for $Re_{2D} \geq 5900$ when these stagnation point average strain rates clearly separate and the following dependence on their length-scales is observed:

$$\frac{\lambda_i}{\lambda_{i+1}} \sim \left(\frac{L_{s_i}}{L_{s_{i+1}}}\right)^{-\alpha} \qquad (1)$$

where α lies between 0.31 and 0.51 for the various values of Re_{2D} above 5900. In fact, there is a tendency for α to decrease with increasing Re_{2D}. As shown in Rossi et al. [13], the energy spectra of the multi-scale flows used here are continuous and scale as $E(k) \sim k^{-p}$ with $p = 2.5$. The value of α consistent with $p = 2.5$ is $\alpha = 0.25$ for a $k^2E(k)$ strain-rate spectrum.

In the vicinity of a steady hyperbolic stagnation point, fluid element pairs of initial separation Δ_0 separate exponentially, i.e. $\Delta(t) \sim \Delta_0 e^{\lambda t}$. To complete the characterisation of our multi-scale stagnation point structure, we estimate the extent of this vicinity, i.e the area of direct influence of each hyperbolic stagnation point. We define this area of influence as the region around $\mathbf{x}_s$ where the velocity field depends linearly on distance from $\mathbf{x}_s$. In suitable eigenframe coordinates, this is the area where $\mathbf{u} \approx \mathbf{u}_s \equiv (\lambda(x - x_s), -\lambda(y - y_s))$. To quantify this area we calculate $Corr \equiv \frac{\mathbf{u}\cdot\mathbf{u_s}}{max(\mathbf{u^2},\mathbf{u_s^2})}$. This quantity $Corr$ is found to fluctuate around a constant value close to or not much smaller than 1 in an area surrounding $\mathbf{x}_s$. Immediately beyond this area, $Corr$ drops off very steeply. This is the area which we interpret as being the area of direct influence of the hyperbolic stagnation point and we plot it in figure 3 for the M_{160} hyperbolic stagnation point and for each of the four M_{40} hyperbolic stagnation points at four different Re_{2D} values.

III. PARTICLE DISPERSION

The Lagrangian trajectories $\frac{d}{dt}\mathbf{x}(t, \mathbf{x}_0) = \mathbf{u_L}(\mathbf{t}, \mathbf{x_0}) = \mathbf{u}(\mathbf{x}(\mathbf{t}, \mathbf{x_0}), \mathbf{t})$ and their statistics are calculated starting from random initial positions $\mathbf{x}_0$ at a time $t = 0$ well after the initial transient caused by the sudden switch-on of the electric field. These trajectories are integrated until $t = 4L_E/u_{rms}$, and we extract statistics of fluid element pair separations $\Delta(t)$, specifically $\overline{\Delta^m}(t)$ for $m = 2, 3, 4, 5, 6$, the averages being carried out over many pairs of fluid elements (more than 10^6).

Pair statistics are initialised with initial separations $\Delta_0 = 1$ *pixel* which is about 25 times smaller than the size of the smallest magnet and therefore smaller than all the length scales of the flow by the size of the smallest magnets). Statistics such as mean square pair separations are sensitive to the choice of Δ_0 but the turbulent diffusivity $\frac{d}{dt}\overline{\Delta^2}$ is much less sensitive as shown recently in [7]. In addition, $\frac{d}{dt}\overline{\Delta^2}$ allows us to clearly identify different dispersion regimes such as the expected initial ballistic dispersion $\overline{\Delta^2} \sim t^2$, the final Brownian dispersion $\overline{\Delta^2} \sim t$ (see [13]) and a non-trivial Richardson-like regime in an intermediate range of times between the ballistic and the Brownian regimes.

Mean square pair separations are plotted in figures 4a and 5b and obey approximate power laws $\overline{\Delta^2} \sim t^\gamma$ for about one decade in time (Re_{2D} large enough). The exponents γ lie roughly between 2 and 3.

In our steady Q2D laminar flows, any mechanism leading to algebraic separation rates with values of γ larger than 2 must necessarily be rooted in the flows's multi-scale stagnation point structure. However, pairs at the vicinity of straining stagnation points separate exponentially. Our measurements of $\partial\overline{\Delta^m}/\partial t$ for $m = 2, 3, 4, 5, 6$ exhibit oscillations in time, which appear weak for $m = 2$

(particularly at the higher Re_{2D} where they hardly appear at all) but are progressively more pronounced as m is made larger, see figure 4. These oscillations can be interpreted as resulting from a sequence of exponential separations $\partial\overline{\Delta^m}/\partial t \propto e^{\beta_m^{(i)}t}$ where $i = 3, 2, 1$ label exponentials in a sequence of three. Indeed, we find that such a sequence of exponentials fits the data well for all values of Re_{2D}. $\beta_m^{(3)}$, $\beta_m^{(2)}$ and $\beta_m^{(1)}$ are well-defined for all m in the respective time ranges 0 to $4/\lambda_3$, $(5-2)/\lambda_2$ to $5/\lambda_2$ and $(8-2)/\lambda_1$ to $8/\lambda_1$. This sequence of exponentials is further corroborated by the finding that (for all Re_{2D}) $\beta_m^{(i)} = m\lambda_{\Delta i}$ where $\lambda_{\Delta i}$ are comparable to the average stagnation point strain rates λ_i. Specifically, $\lambda_{\Delta 3}/\lambda_3$ is about 1, $\lambda_{\Delta 2}/\lambda_2$ is about 0.8, $\lambda_{\Delta 1}/\lambda_1$ is about 0.4, with standard deviation 0.1 across Reynolds numbers.

These findings suggest that, over the entire range of Reynolds numbers, pairs separate on average as a result of successive exponential straining actions by the stagnation points directly imposed by the three scales of EM forcing. The fact that the exponential separation rates appear in sequence with exponents closely related to the average stagnation point strain rates λ_i suggests a Richardson-like locality. The pair separation rate is first imposed by the "smallest" straining stagnation points corresponding to L_{s3}, then by the intermediate straining stagnation points corresponding to L_{s2} and finally by the "largest" stagnation point which corresponds to L_{s1}. Hence, the multi-scale stagnation point structure of our flows drives pair diffusion in a Richardson-like manner. The oscillations superimposed on this behaviour are weaker as Re_{2D} increases because the multi-scale nature of distinct and ordered strain rates are better defined (see model calculation in [13] where it is shown that a succession of exponentials can give rise to power-law growth).

In the light of these results and conclusions we do not claim that $\overline{\Delta^2}$ has an exact power-law dependence on time. However, as argued in [5] and [13], a statistical sequence of exponential separation events (where pairs stay together for long and then suddenly separate) can integrate into an approximate power-law time-dependence of $\overline{\Delta^2}$. Indeed, the data are well fitted by $\overline{\Delta^2} \sim t^\gamma$ over nearly a decade of times bounded from above by $2L_E/u_{rms}$. The values of γ are given in Figure 5 as function of Re_{2D}. They are extracted from best power law fits of $\frac{d}{dt}\overline{\Delta^2}$ over the range $0.2 \leqslant tu_{rms}/L_E \leqslant 2$.

The values of γ are found to increase with Re_{2D} whilst the topology of the flow does not change significantly: there is no increase in the number of stagnation points nor a systematic increase of the stagnation points's area of influence (Figure 3). This increase of γ towards an approximately constant value beyond $Re_{2D} \approx 5900$ is correlated with a steep decrease of the ratio of the large-scale turnover time, L_E/u_{rms}, to the bottom friction's viscous time, H^2/ν (see Figure 5). This ratio reaches 1 at $Re_{2D} \approx 5900$ and is smaller for larger values of Re_{2D}. Hence, the Re_{2D} independent value of γ is reached once the bottom friction has been overcome by the EM forcing.

IV. CONCLUSION

It is perhaps an amusing coincidence that this asymptotic value of γ is close to 3, which is the value predicted for and observed in isotropic homogeneous turbulence [3, 8–10]. It is nevertheless striking that our pair separation statistics exhibit Richardson-like locality and $\overline{\Delta^2} \sim t^\gamma$ with $\gamma \approx 3$ even though our flows are laminar, steady and Q2D. As shown in section II, a power-law multi-scale distribution of stagnation point strain rates is fully achieved only when $Re_{2D} \geq 5900$ which perfectly corresponds with the onset of a constant γ value close to 3 and a bottom friction that has been overcome by the EM force field. Only at such high values of Re_{2D} are the stagnation point strain rates clearly distinct and ordered by stagnation point length-scales (themselves ordered in approximate proportion to magnet sizes irrespective of Re_{2D}) according to (1). Note that the variations in γ are correlated with redistributions of the three stagnation point strain rates relative to each other (figure3). We observe a maximum γ of about 3.2 ($Re_{2D} = 7400$) in the case where (1) fits the data best.

Funds: The Leverhulme Trust, Royal Society, EPSRC.

[1] L. F. Richardson, Proc. R. Soc. Lond. A **110**, 709 (1926).
[2] J. C. H. Fung, J. C. R. Hunt, N. A. Malik, and R. J. Perkins, J. Fluid Mech. **236**, 281 (1992).
[3] M. C. Jullien, J. Paret, and P. Tabeling, Phys. Rev. Lett. **82**, 2872 (1999).
[4] J. C. H. Fung and J. C. Vassilicos, Phys. Rev. E **57**, 1677 (1998).
[5] S. Goto and J. C. Vassilicos, New J. Phys. **6**, 1 (2004).
[6] J. Davila and J. C. Vassilicos, Phys. Rev. Lett. **91**, 144501 (2003).
[7] F. Nicolleau and G. Yu, Phys. Fluids **16**, 2309 (2004).
[8] S. Ott and J. Mann, J. Fluid Mech **422**, 207 (2000).
[9] G. Boffetta and I. M. Sokolov, Phys. Rev. Lett. **88**, 094501 (2002).
[10] T. Ishihara and Y. Kaneda, Phys. Fluids **14**, L69 (2002).
[11] S. Goto, D. R. Osborne, J. C. Vassilicos, and J. D. Haigh, Phys. Rev. E **71**, 015301 (2005).
[12] J. C. Vassilicos, J. Davila, S. Goto, E. Hascoet, D. R. Osborne, and L. Rossi, Proc. IUTAM Symp. on Elementary Vortices and Coherent Structures: Significance in Turbulence Dynamics, ed. S. Kida, Springer. (2006).
[13] L. Rossi, J. C. Vassilicos, and Y. Hardalupas, J. Fluid Mech. **558**, 207 (2006).
[14] J. M. Ottino, Cambridge University Press (1989).